J Solid State Eletrochem (2004) 8: 416–421
DOI 10.1007/s10008-003-0444-2

ORIGINAL PAPER

R. Ramanauskas · R. Juškėnas · A. Kaliničenko
L. F. Garfias-Mesias

Microstructure and corrosion resistance of electrodeposited zinc alloy coatings

Received: 19 May 2003 / Accepted: 4 August 2003 / Published online: 22 October 2003

Abstract A heat treatment effect on the microstructure and corrosion properties of electrodeposited Zn, Zn-Co, Zn-Fe and Zn-Ni alloy coatings was studied. Surface morphology examinations were carried with AFM, while XRD was used to determine metal lattice parameters, texture and phase composition. Low-temperature annealing (at 225 °C) caused the formation of intermetallic Fe/Zn compounds, a transformation of amorphous oxide inclusions to the crystalline form and a decrease in the Zn lattice parameter for Zn-Co and Zn-Fe alloys. The mentioned structural modifications were not accompanied, however, by corrosion behavior changes of these coatings. On the Zn-Ni alloy, the annealing caused a significant reduction in the diffraction peak width and simultaneous considerable augmentation of the corrosion current. This effect is related to the formation of a less disordered lattice for this alloy.

Keywords Corrosion · Heat treatment · Microstructure · Zinc alloys

Introduction

Electrodeposited Zn alloys with Fe group metals have been shown to significantly extend the corrosion protection of steel with respect to conventional Zn coatings. The highest corrosion resistance is achieved when Co or Fe in the alloy is less than 1 wt% and the amount of Ni is within 9–15 wt% [1, 2, 3, 4, 5, 6, 7, 8, 9, 10, 11, 12, 13, 14]. Alloying with Zn confers sufficient corrosion resistance to steel that nowadays it is a common procedure for most industries, particularly the automotive industry [1, 15].

Differences between the corrosion behaviour of electrodeposited Zn and Zn alloys in natural atmospheric conditions and in some aqueous solutions were reported in recent studies [11, 12, 13, 14]. It was established [11] that these differences manifest themselves when a passivating oxide film forms on the metal surface. It was also suggested that the metal structural parameters, especially lattice imperfections, were responsible for the corrosion behaviour of the investigated coatings [11].

Metal dissolution is known to occur mainly at surface-active sites where atoms are weakly bonded to the crystal surface [16]. The number of such active sites and, hence, their relative importance to the corrosion reaction rate, is dependent on the surface crystallography (nanometer level) and surface topography (10–100 nm level) [16, 17]. However, the lack of experimental evidence regarding the influence of the structural parameters on the corrosion behaviour of Zn and Zn-alloyed coatings requires additional studies.

Low-temperature annealing enables avoidance of grain growth and texture transformation; therefore, this procedure would allow verification of the role of lattice defects in the corrosion process. This ''mild'' heat treatment (at low temperatures) is thought to simulate the corrosion conditions under which some Zn-electroplated compounds are subjected in real life applications (e.g. in the car engine compartment). Most of the literature on this topic [18, 19] deals with chromated coatings and mostly tries to understand the severe heat treatment influence on chromate film properties. Siluvai and Radhakrishna stated [19] that the heat treatment induces a noticeable decrease in the resistance of chromated Zn against white rust, while the corrosion

Contribution to the 3rd Baltic Conference on Electrochemistry, GDAŃSK-SOBIESZEWO, 23–26 APRIL 2003.

Dedicated to the memory of Harry B. Mark, Jr. (February 28, 1934–March 3rd, 2003)

R. Ramanauskas (✉) · R. Juškėnas · A. Kaliničenko
Institute of Chemistry, A. Goštauto 9,
2600 Vilnius, Lithuania
E-mail: ramanr@ktl.mii.lt
Tel.: +370-5-2610067
Fax: +370-5-2617018

L. F. Garfias-Mesias
Lucent Technologies, SCN,
600 Mountain Avenue,
Murray Hill, NJ 07974, USA

behaviour of the chromated Zn-Ni alloys remains unchanged.

The main goal of the present work was to establish the influence of low-temperature annealing on the structural parameters and corrosion behaviour of Zn and Zn-alloy coatings. The main techniques used in these studies were X-ray diffraction, atomic force microscopy and DC electrochemical methods.

Experimental

Pure zinc coating on steel was compared to three Zn alloys: Zn-Co (0.6%), Zn-Fe (0.4%) and Zn-Ni (12%) coatings of 10 μm thickness, which were electrodeposited on low-carbon steel samples. These concentrations of the alloying elements were chosen at just below the limit concentration for proper solubility (Zn-Co and Zn-Fe alloys) and for formation of the desired phase composition (γ-$Zn_{21}Ni_5$). The carbon steel bars were previously polished mechanically to a bright mirror finish using 0.3 μm alumina powder. Alkaline cyanide-free plating solution contained ZnO (10 g/L), NaOH (100 g/L), organic additives and the ions of the alloying elements. The plating bath detailed composition and operating conditions have been given in a previous publication from our group [12].

XRD measurements were carried out with a DRON diffractometer using Cu K_α radiation selected by a secondary graphite monochromator. The step scan mode with a step size of 0.05° (2Θ) and a sampling time of 20 s/step were used in the range of $30° \leq 2\Theta \leq 75$.

AFM studies were carried out with an Explorer (VEECO Thermomicroscopes) scanning probe microscope at atmospheric pressure and room temperature in contact mode.

The corrosion behaviour of the coatings was investigated in 0.1 M NaCl + 0.1 M $NaHCO_3$ solution (pH 6.8) using a standard three-electrode system. The cell was composed of the working electrode (Zn-alloyed steels), a Pt counter electrode and a saturated calomel reference electrode using a PI 50-I potentiostat.

Sample annealing was performed during 8 h at 225 °C under vacuum ($\sim 10^{-3}$ Torr).

Results

XRD studies

The heat treatment temperatures (t°), which were applied for Zn and Zn-alloy coatings, varied between 200 °C and 300 °C. Annealing at t° lower than 200 °C caused no changes in the XRD patterns of the investigated samples, even for a longer treatment period (48 h). At t° higher than 200 °C the development of additional peaks, corresponding to intermetallic Zn/Fe compounds, was observed (Fig. 1). The formation of this phase occurs due to interdiffusion in the interface region between the Zn and the steel substrate. The main idea of our study was to change the structure, but not the composition, of the investigated coatings. Therefore, the development of this phase in a considerable amount was not desirable; hence, annealing at t° equal to 225 °C was applied for this study.

Figure 1 shows typical XRD patterns for all samples before heat treatment (dotted lines) and after annealing in vacuum at 225 °C for 8 h (solid lines). The as-deposited pure Zn coating showed sharp peaks corresponding to Zn and α-Fe (Fig. 1a). The annealing process of this coating did not change the characteristic 2Θ values for the Zn peaks. However, several additional peaks appeared after heat treatment in vacuum. One of them may be attributed to ZnO ($d = 1.625$ Å) and others correspond to a Zn/Fe intermetallic phase. A full-width-at-half-maximum (FWHM), W_{FWHM}, was derived for the Zn (110) peaks as deposited and for that after annealing; the obtained values appeared to be very similar, 0.494 and 0.492, respectively.

The XRD patterns corresponding to Zn-Co and Zn-Fe samples are shown in Fig. 1b and Fig. 1c, respectively. Annealing, similar to pure Zn, caused the formation of the intermetallic ξ-$FeZn_{15}$ phase and the appearance of an additional peak, corresponding to ZnO. In contrast to the previous coating, the ZnO phase, shown as a broad peak at 56°, was found in the annealed Zn-Co and Zn-Fe alloys in a considerable amount (8–10 at%). Both of these coatings were strongly oriented in the direction $<110>$ (as shown by the large peak found at ~70° 2Θ). After heat treatment, two representative peaks of Zn (100 and 110) were shifted towards higher 2Θ angles; this is indicative of a decrease of the Zn lattice parameter a. The latter effect may be caused by formation of a substitutional solid solution instead of interstitial one, which was present in the as-deposited Zn-Co and Zn-Fe coatings. A slight decrease of W_{FWHM} values was observed after the heat treatment of these coatings as well. W_{FWHM} of the Zn (110) peak for the as-deposited Zn-Co coating reduced from 0.539 to 0.491; for the Zn-Fe sample the W_{FWHM} values were as follows: 0.524 for the as-deposited and 0.495 for the annealed coatings. The peak $d = 1.280$ Å, which appears after annealing of Zn and low alloyed Zn coatings with Co and Fe, belongs most probably to the intermetallic ξ-$FeZn_{15}$ phase (PDF No. 34-1314).

The as-deposited Zn-Ni coating showed two peaks in the XRD pattern in the 2Θ range studied: a broad peak with a d value of 2.101 Å, corresponding to the γ-Zn-Ni phase, and a peak next to it corresponding to α-Fe(110) (Fig. 1d). Pure Zn and low-alloyed coatings with Co and Fe electrocrystallize with a distorted form of hexagonal close packing; Zn-Ni possesses a body-centred cubic crystal system. Several additional peaks appeared after annealing; these peaks could be attributed to the γ phase of the Zn-Ni alloy and an intermetallic phase of ϵ-$Zn_{10}Fe_3$, which forms at the coating/substrate interface. A small peak for ZnO ($d = 1.622$ Å) can be seen on the pattern of the annealed Zn-Ni coating. The annealing of these coatings caused a significant decrease in the W_{FWHM} value, from 0.744 to 0.428.

Surface morphology studies

The influence of heat treatment on the surface morphology can be observed in the AFM images, which

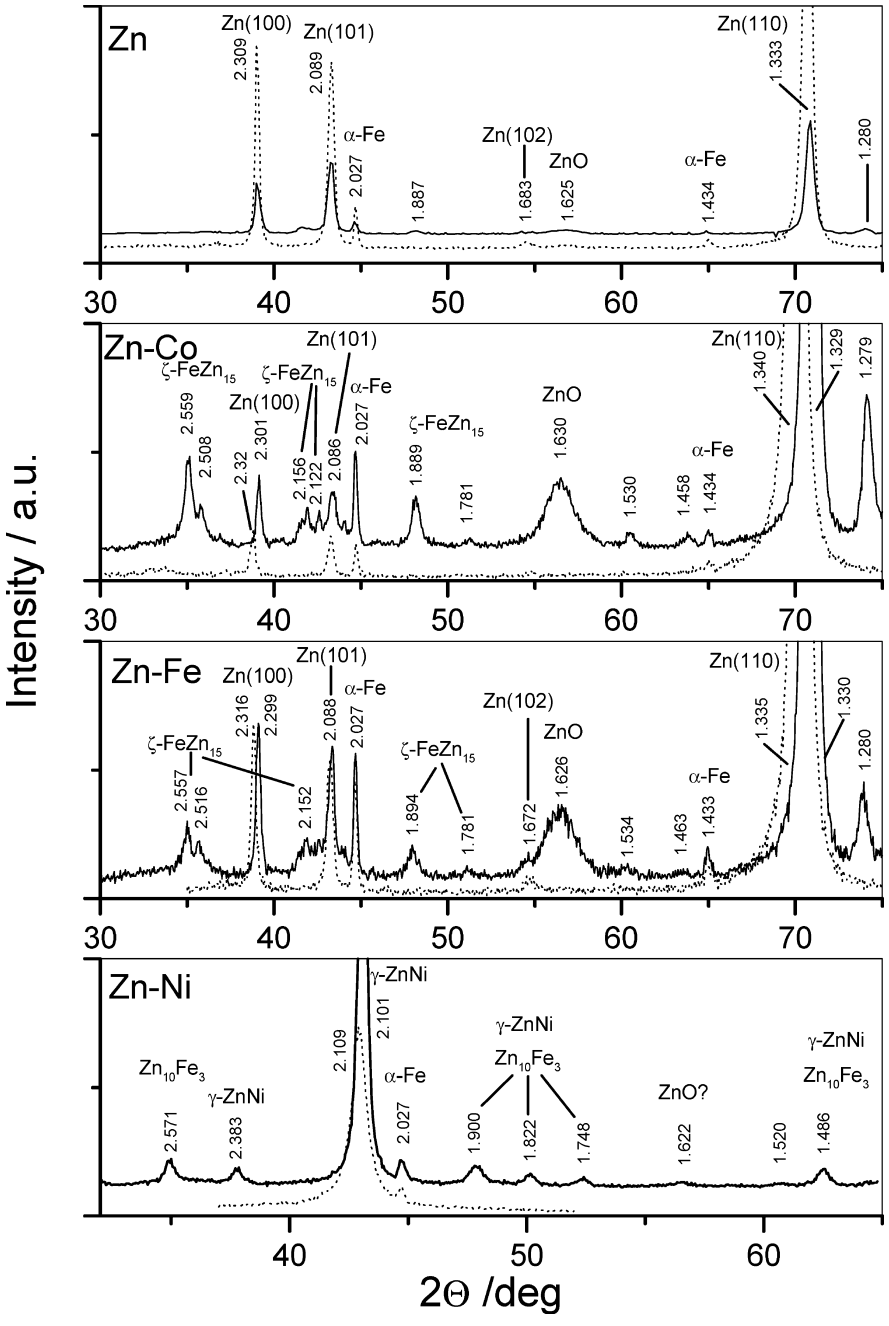

Fig. 1 X-ray diffraction patterns of Zn coatings as-deposited (*dotted line*) and after annealing (*solid lines*) in vacuum at a temperature of 225 °C for 8 h

are shown in Fig. 2. The AFM image shows a 20×20 μm area with the height represented by the greyscale bar that appears on the left of each image. All the images that appear in the left side of Fig. 2 show the surface morphology of all the samples after electrodeposition. Zinc, Zn-Fe and Zn-Co samples appeared finely grained with pyramidal-shaped crystals [11]. These coatings were bright, compared to Zn-Ni, which were dull in appearance. The Zn-Ni sample has a different structure from the rest of the coatings (i.e. a nodular fine grained morphology) [11].

The same scanned areas shown on the left side of Fig. 2 were re-scanned again after annealing and are shown on the right side of Fig. 2. The values of the surface root-mean-square roughness (R_{rms}) are shown underneath every image. The surface topography of the investigated coatings does not undergo significant modifications during the sample thermal treatment. It can be observed that the same features that appear prior to annealing are shown in the post-annealed sample. R_{rms} values before and after heat treatment are within the error margins for Zn and alloyed coatings. Therefore, based upon the minimal change of the surface roughness, we expect that this annealing did not cause a significant change in the crystal shape of the investigated coatings.

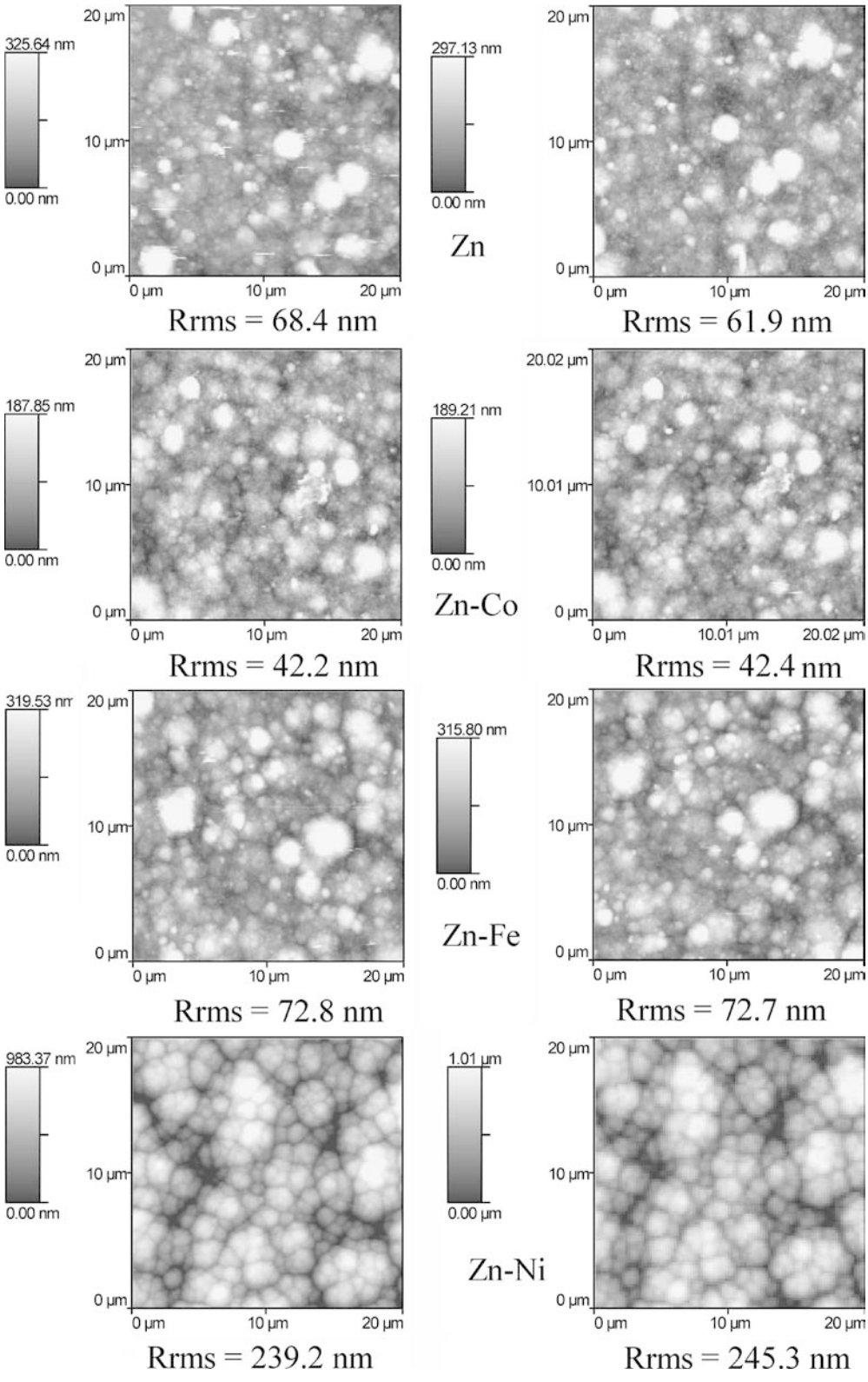

Fig. 2 AFM images of Zn and Zn alloys electrodeposited before thermal treatment (*left*) and after thermal treatment (*right*)

Electrochemical measurements

Corrosion currents were determined from polarization measurements in a $NaCl + NaHCO_3$ solution before and after sample annealing. Zn corrosion in unbuffered Cl^- solution occurs with oxide/hydroxide film formation, which possesses a porous structure [20]. However, in HCO_3^- containing media the oxide film is supposed to be more compact, adherent and less soluble, thus exhibiting a passivating character [21]. Aqueous corrosion data for Zn

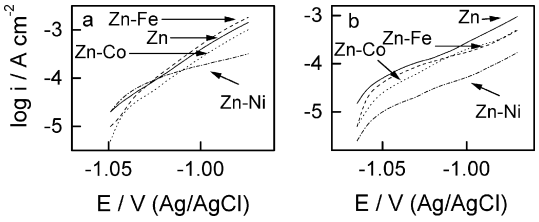

Fig. 3 Anodic polarization curves of Zn and Zn-alloy samples in 0.1 M NaCl + 0.1 M $NaHCO_3$ solution before (**a**) and after (**b**) heat treatment. Potential scan rate: 0.1 mV s^{-1}

and Zn alloys in HCO_3^- containing media correlate well with the atmospheric corrosion data obtained in the field [11, 12]. Anodic polarization curves of the investigated samples are presented in Fig. 3.

The corrosion current densities were determined from Tafel plot extrapolation. They were obtained from a computer fit to the data and, together with the values of the corrosion potentials, are listed in Table 1. In spite of the structural changes of the Zn-Co and Zn-Fe coatings induced by annealing, these alloys exhibited very similar E_{corr} and i_{corr} values for both the as-deposited and annealed samples. A small reduction of i_{corr} from 5.5 to 3.1×10^{-5} A cm^{-2} was observed for pure Zn coatings as the result of the same treatment. Meanwhile, the effect of annealing on the corrosion behavior appeared to be significant for the Zn-Ni coating. The E_{corr} values of the heat-treated Zn-Ni sample became ~10 mV more negative with respect to the untreated coating; however, the i_{corr} values increased considerably. For the as-deposited coating, i_{corr} was of the order 6.2×10^{-6} A cm^{-2}, while for the annealed sample i_{corr} was 3.9×10^{-5} A cm^{-2}.

Discussion

The corrosion process is essentially a surface phenomenon; thus it might be strongly related to crystalline imperfections. Highly stepped metal surfaces, with dislocations, make the steps indestructible. The importance of steps and kinks in lowering the activation energy of corrosion has been long recognized [17].

It is well known that annealing of metals enhances structural changes and reduces the number of lattice defects [22, 23]. Therefore, the heat treatment procedure is a suitable method for determining the surface structure relationship with the kinetics of corrosion reactions.

The heat treatment applied in this investigation did not produce any significant changes on the Zn and Zn-alloy surface morphology; however, it caused formation of intermetallic Zn/Fe compounds due to interdiffusion at the coating/substrate interface. The latter phase was located at the mentioned interface and appeared to have no influence on the corrosion currents of the investigated coatings. The following consequence of the heat treatment was the appearance of a peak on the XRD pattern, corresponding to ZnO. The annealing was carried out under low vacuum conditions; hence, the oxide phase formation resulting from the metal contact with the ambient oxygen, apart from being a thin film of oxide, could be most likely confined to the surface. Therefore, after the samples were heat treated and etched (in order to remove oxide from the surface), the corresponding ZnO peak remained on the XRD patterns. This fact implies that the oxide was located not only on the sample surface, but also in the bulk of it.

The Zn electrodeposition process from alkaline solutions occurs through Zn hydroxide inclusion formation [5, 24, 25]. The amount of such inclusions according to some data [5] can account up to 18% of the total Zn coatings mass. Our previous results have shown [25] that the difference in the corrosion behaviour of the coatings investigated here cannot be associated with the non-metallic inclusions. The XRD did not detect this phase before heat treatment, suggesting that oxide inclusions are in an amorphous state. Therefore, the appearance of an oxide peak after the sample was annealed suggests the transformation of the amorphous to the crystalline oxide phase. However, this transformation, which was more pronounced for Zn-Co and Zn-Fe alloys, appeared to have no influence on the corrosion properties of the coatings.

The heat treatment caused the decrease of the Zn lattice parameter *a* for the same low-alloyed Zn coatings with Co and Fe; this is probably related to the transformation of an interstitial solid solution to substitutional one. However, these changes were also not found to be associated with the corrosion properties of the alloys (i.e. changes in E_{corr} or i_{corr}).

Similar to the other coatings, the heat treatment of Zn-Ni alloy caused the formation of an intermetallic and transformation of the oxide phases. However, both these structural modifications have little effect on the corrosion behaviour (Zn-Co and Zn-Fe examples). This increase in the corrosion current of Zn-Ni (after annealing) may be related to the decrease of the diffraction line width (W_{FWHM}). X-ray diffraction line broadening of metals is recognized to be caused by crystallite size and lattice strains [26, 27]. In general, the grain size of the

Table 1 Corrosion potentials and currents of Zn and Zn-alloy samples in 0.1 M NaCl + 0.1 M $NaHCO_3$ solution before and after heat treatment

Sample	Before annealing		After annealing	
	E_{corr} (V) (Ag/AgCl)	i_{corr} (A cm^{-2})	E_{corr} (V) (Ag/AgCl)	i_{corr} (A cm^{-2})
Zn	−1.066	5.5×10^{-5}	−1.060	3.1×10^{-5}
Zn-Co	−1.050	1.0×10^{-5}	−1.051	1.5×10^{-5}
Zn-Fe	−1.056	1.8×10^{-5}	−1.055	1.4×10^{-5}
Zn-Ni	−1.045	6.2×10^{-6}	−1.055	3.9×10^{-5}

investigated Zn and Zn-alloy electrodeposits lies in the range 0.1–2 μm, for which X-ray diffraction is quite insensitive [28, 29]. Hence, the changes in W_{FWHM} for the investigated Zn coatings will be affected mostly by the changes in their lattice imperfection.

The W_{FWHM} changes imply formation of a less disordered lattice of the alloy during annealing. Meanwhile, the augment of the i_{corr} values supports the idea that the more disordered lattice of the Zn alloy finally yields lower corrosion rates for the Zn alloy coating. The more disordered lattice of the Zn alloy increases the surface activity for oxide film formation and affects the oxide film properties [11]. A higher surface activity of Zn-Ni alloys, and hence the metal structure, may be the precursor to the formation of the oxide film, which contains a large amount of Zn hydroxide and exhibits a poor crystallinity [11]. An amorphous structure and less electron conductivity of hydrated Zn oxide with respect to Zn oxide [3] makes such alloys more stable in corrosion environments where a passive film forms on the metal surface.

The role of the oxide non-metallic inclusion on the corrosion behaviour of Zn and Zn-alloy coatings, deposited from alkaline solutions, needs to be studied in detail in the future.

Conclusions

Low-temperature annealing of Zn, Zn-Co, Zn-Fe and Zn-Ni electrodeposited coatings did not produced major changes in their morphology; it caused the formation of intermetallic Fe/Zn compounds, transformation of amorphous oxide inclusions to the crystalline form and a decrease of the Zn lattice parameter a for the low-alloyed Zn-Co and Zn-Fe coatings. These structural changes, however, were not accompanied by changes in the sample corrosion currents. A significant reduction of the diffraction line width was observed for the Zn-Ni alloy. A substantial increase in the Zn-Ni alloy corrosion rates after annealing is related to the formation of a more ordered lattice for this alloy.

References

1. Loar GW, Romer KR, Aol TJ (1991) Plat Surf Finish 78:74
2. Shears AP (1989) Trans Inst Met Finish 67:67
3. Wilcax GD, Gabe DR (1993) Corros Sci 35:1251
4. Sizelove RR (1993) Plat Surf Finish 78:26
5. Baldwin KR, Robinson MJ, Smith CJE (1993) Corros Sci 35:1267
6. Fedrizzi L, Fratesi R, Lunazzi G, Roventi G (1992) Surf Coat Technol 53:171.
7. Stankevičiūtė A, Leinartas K. Bikulčius G, Virbalytė D, Sudavičius A, Juzeliūnas E (1989) J Appl Electrochem 28:89
8. Alfantazi AM, Erb U (1996) Corrosion 52:880
9. Bajat JB, Maksimivic MD, Miškovic-Stankovic VB, Zec S (2001) J Appl Electrochem 31:355
10. Ivanov I, Valkova T, Kirilova I (2002) J Appl Electrochem 32:85
11. Ramanauskas R (1999) Appl Surf Sci 153:53
12. Ramanauskas R, Muleshkova L, Maldonado L, Dobrovolskis P (1998) Corros Sci 40: 402
13. Ramanauskas R, Quintana P, Bartolo-Perez P, Diaz-Ballote L (2000) Corrosion 56:588
14. Ramanauskas R, Gudaviciute L, Diaz-Ballote L, Bartolo-Perez P, Quintana P (2001) Surf Coat Technol 140:109
15. Zaki N (1989) Met Finish 87: 57
16. Vela ME, Andreasen G, Aziz SG, Salvarezza RC, Arvia AJ (1998) Electrochim Acta 43:3
17. Fernandes MG, Latanision RM, Searson PC (1993) Phys Rev B 47:11749
18. Fedrizi L, Fratesi R, Lunazzi G, Roventi G (1992) Surf Coat Technol 53:171
19. Siluvai M, Radhakrishna S (1998) Anti-Corros Methods Mater 45:113
20. Gradel TE (1989) J Electrochem Soc 136:193C
21. Guo R, Weinberg F, Tromans D (1995) Corrosion 51:356
22. Martyak NM, Wetterer S, Harrison L, McNeil M (1994) Met Finish 92:111
23. Afseth A, Nordlien JH, Scamans GM, Nisancioglu K (2002) Corros Sci 44:145
24. Yan H, Downes J, Boden PJ, Haris SJ (1996) J Electrochem Soc 143:1577
25. Ramanauskas R, Jureviciute I, Selskis A (1998) Chem J Lith Acad Sci 4:291
26. De Keijser ThH, Langford JI, Mittemeijer EJ, Vogels ABP (1982) J Appl Crystallogr 15:308
27. Balzar DJ (1992) J Appl Crystallogr 25:559
28. Cullity BD (1978) Elements of X-ray diffraction, 2nd edn. Addison-Wesley, Reading, Mass., USA
29. Van Berkum JGM, Delhez R, De Keijser ThH, Mittemeijer EJ (1996) Acta Crystallogr Sect A 52:730